

Response of low latitude ionosphere to the space weather event of November 2012 in the Asian Sector

Shivalika Sarkar^{a*}, Shweta Mukherjee^b & A.K. Gwal^c

^aRegional Institute of Education, Shyamla Hills, Bhopal 462002, India

^bVIT Bhopal University, Kothri, Bhopal 466114, India

^cRabindra Nath Tagore University, Bhopal Chiklod Road, Raisen 464993, India

Received 9 December 2017; Accepted 22 August 2019

Ionospheric response to geomagnetic storms is determined by the efficiency of the solar wind-magnetosphere-ionosphere coupling that underlies the transfer of tremendous amount of mass and energy. A study was carried out to see the response of the equatorial and low latitude ionosphere to the moderate geomagnetic storm of 14 November 2012. This study was carried out using vertical total electron content (VTEC) measured by Global Positioning System (GPS) receivers along the $\sim 115^\circ$ - 121° E longitude. The GPS TEC observations showed pronounced positive storm effects in the Asian sector ($\sim 115^\circ$ - 121° E) during the main phase of the storm, for the low latitude and crest of anomaly stations. During the main phase of the storm, the interplanetary electric field (IEF) penetrated to the equatorial ionosphere and caused significant density changes in the equatorial ionization anomaly (EIA) region. The eastward prompt penetration electric field, associated with southward interplanetary magnetic field (IMF) augmented the normal daytime eastward dynamo electric field, resulting in intensification of equatorial ionization anomaly (EIA) and VTEC enhancements observed over the anomaly crest stations. Results showed that EIA region was significantly affected during geomagnetic storms in comparison to the low latitude ionosphere.

Keywords: Ionosphere, Geomagnetic storm, GPS, Total Electron Content

1 Introduction

Ionosphere is the charged layer of the upper atmosphere which responds markedly to varying solar and magnetospheric energy inputs. During a geomagnetic storm, the solar wind energy deposited into the magnetospheric polar cap region will eventually be dissipated into the ionosphere and thermosphere. Meanwhile, various physical and energy transport processes within the ionosphere become extreme and more complicated¹⁻³. A geomagnetic storm is a dynamic process that involves dramatic changes in the magnetosphere, bringing changes in the earth's magnetic field. Coupling process between ionosphere and magnetosphere is complex and highly variable. There is flow of mass, momentum and energy into and through the magnetosphere-ionosphere system. There can be large changes in the altitude and horizontal distribution of plasma density, temperature, ion composition, conductivity of the high latitude thermosphere-ionosphere system which in turn significantly affects the global thermosphere-ionosphere system through various processes.

Electric fields can produce rapid ion drifts, plasma outflows, ion temperature increases, deep ionization troughs and chemical changes in the ionosphere. The neutral atmosphere is also affected by energetic inputs from magnetosphere. Both chemical and dynamical changes lead to variation in neutral density. The ionosphere carries the coupling current system and provides feedback to the magnetosphere in the form of ion outflow, conductivity changes and dynamo electric fields. Hence there can be changes in neutral composition, neutral winds, electric fields and other horizontal transport. The observed storm effects at a given location may be the effect of a combination of these mechanisms. Over the equatorial and low latitudes the consequent thermospheric and electric field disturbances are indirect.

Interactions of the various near Earth space plasma regions with the interplanetary magnetic field and solar wind has been known for decades. Various aspects of this process continue to attract intensive research even today. Ionospheric storms occur in response to geomagnetic storms and represent an extreme form of 'space weather' which can have significant, adverse effects on increasingly

*Corresponding author (E-mail: shivalikasarkar@gmail.com)

sophisticated ground and space based systems. Solar disturbances can produce prompt and delayed effects at Earth. In particular, one of the major indications of the magnetosphere ionosphere coupling is the significant variation of electron density during a storm^{4,5}.

However, some features of this phenomenon are still not clear and remain hardly predictable, e.g. strong longitudinal and latitudinal asymmetries, alternation of positive and negative phases or the completely different storm-induced disturbance behavior of the ionospheric F2 region above two comparable locations which are frequently observed⁶⁻⁸.

The equatorial region involves a complex interplay between aeronomic, electrodynamic and plasma physical processes. At dawn and throughout the daytime hours, sunlight illuminates the atmosphere, both heating and photoionizing atoms and molecules. Thermal expansion of the atmosphere leads to upward motion of the neutrals and strong neutral-ion collisions drag the ions along with the neutrals. The upward motion of ionospheric ions and electrons at the dip equator can also be thought of as the presence of an eastward electric field associated with $E \times B$ drift of the plasma. Eastward electric fields exist during the day in the equatorial region, thereby producing an upward plasma drift. The plasma lifted then diffuses down the magnetic field line and away from the equator. Plasma located slightly away from the equator is not only lifted upward but also displaced to higher latitudes. A dynamic equilibrium between $E \times B$ forces, gravitational forces and photoionization and recombination lead to ionospheric density enhancements located at $\sim \pm 15^\circ$ from the equator during geomagnetically quiet times. These latter maxima are called the Equatorial Ionospheric Anomalies or EIAs⁹. This overall process of plasma uplift and the formation of the EIAs away from the equator is called the "fountain effect" since the plasma flow is like a fountain. The study of F region multiple stratifications can reveal the ionospheric electrodynamics and day to day variability of the equatorial and low latitude region¹⁰. Magnetic storms can produce large and complex electrodynamic disturbances in the equatorial ionosphere and can cause modification of the equatorial fountain.

The solar wind interplanetary electric field (IEF) can interact with the equatorial ionospheric electric fields and are known as prompt penetration electric fields (PPEF) if there is an immediate response of

ionospheric electric fields to a variation of IEF. According to Fejer¹¹, PPEF occurs during periods of large and rapid IMF driven changes in magnetospheric convection, when there is a temporary imbalance between the convection-related charge density and the charge density in the Alfvén layer. As shown by numerous modeling studies, the morphology and physics of equatorial prompt penetration electric fields are far more complex than implied by simple proportionality factors between the either the magnitudes or the time rate of changes of equatorial and solar wind electric fields^{12,13}. These studies have shown that the prompt penetration effects are driven by the solar wind and magnetospheric driving mechanisms, but that their strength, duration and local time dependence are controlled by the potential distribution penetrating to middle and low latitudes, which depend on magnetospheric parameters such as the equivalent ring current conductivity (proportional to the plasma sheet temperature and density), and on ionospheric conductances. During day time, prompt penetration electric field is eastward and enhances the dynamo electric field. This dynamo electric field enhances vertical $E \times B$ plasma drift with lifting the plasma to higher altitudes¹⁴. At these altitudes, the production to loss ratio is greater which results into enhanced electron density in the dayside sector. Thus prompt penetration electric field is associated with huge enhancement in TEC in the dayside sector¹⁵ and depletion in TEC in night side sector¹⁶. The EIA is also found to intensify in amplitude and latitude extent in the presence of PPEF¹⁷. Huang¹⁸ suggested that IEF can continuously penetrate to the low latitude ionosphere without shielding during storm periods of strengthening geomagnetic activity. Several studies have investigated the properties of the equatorial ionosphere with specific attention to longitudinal variations in the properties of the plasma. The global distribution of vertical plasma drifts was examined by Fejer¹⁹, using data from the AE-E satellite. Gaurav²⁰ studied the effect of the geomagnetic storm on the equatorial ionization anomaly (EIA) and equatorial temperature anomaly (ETA) using the atomic oxygen day glow emissions at 577.7 nm (OI 577.7 nm) and 732.0 nm (OII 732.0 nm) for four intense geomagnetic storms during the ascending phase of solar cycle 24. The EIA crests were found to show poleward movement in the higher altitude regions. The volume emission rate of 732.0 nm emission showed a strong

enhancement during the main phase of the storm. A chain of GPS receivers can be helpful in understanding the ionospheric dynamics from the equatorial to the low latitude region. In this paper we discuss the response of ionosphere to the moderate geomagnetic storm of 14 November 2012 using TEC data obtained from several stations in the Asian Sector. These stations lie in the equatorial ionization anomaly (EIA) and low latitude region in both the northern and southern hemispheres. Effects of the storm on different latitudes are studied and the underlying physical mechanism is also investigated.

2 Data and Methodology

For studying the characteristics of the geomagnetic storm of 14 November, 2012 and its coupling with magnetosphere, we have collected the solar wind speed and z component (B_z) of the interplanetary magnetic field (IMF), the planetary index (kp), mean, 3-hourly equivalent amplitude of geomagnetic activity (A_m) and auroral electrojet index (AE). For studying the ionospheric response to this geomagnetic storm, we collected TEC data from stations shown in Fig. 1. Coordinates of the stations are provided in Table 1. Solar data (Solar wind speed and B_z IMF) were downloaded from spaceweather.com. Geomagnetic data (kp , am and AE) were downloaded from <http://spidr.ngdc.noaa.gov/spidr>. Calibrated TEC data were downloaded from the website <http://tict4d.ictp.it/nequick2/gnss-tec-calibration>. In addition we have also collected the data from Thermosphere, Ionosphere, and Mesosphere, Energetics and Dynamics (TIMED) spacecraft which orbits at 630 km altitude with an inclination of 74.1° ²¹. The TIMED/GUVI stands for the Global Ultraviolet Imager (GUVI) instrument onboard the TIMED satellite. As described by Yee²² the GUVI instrument provides spatial and temporal variations of constituent number densities and temperature in the thermosphere. According to Yee²³, GUVI is a spatial scanning imaging spectrograph designed to observe the sources of the far ultraviolet (FUV)

airglow emissions in the Earth's upper atmosphere. It was designed to provide cross-track scanned images of these FUV emissions at wavelengths ranging from 115 to 180 nm, including the major emission features of hydrogen's (H) Lyman- line, atomic oxygen (O) emission lines, and molecular nitrogen (N₂) Lyman Birge-Hopfield (LBH) bands. A typical GUVI orbit includes day, night and auroral observations. Successive orbits provide overlapping coverage at the poles and nearly continuous coverage at the equator. GUVI monitors three general regions on each orbit: the daytime low- to mid-latitude thermosphere, the night time low- to mid-latitude ionosphere and the high-latitude auroral zone. The instrument's data products are maps of the characteristics of the ionosphere and thermosphere, including maps of the auroral oval, the characteristic energy and flux of the electrons that excite it, F-region (≈ 160 – 400 km) ionospheric electron density

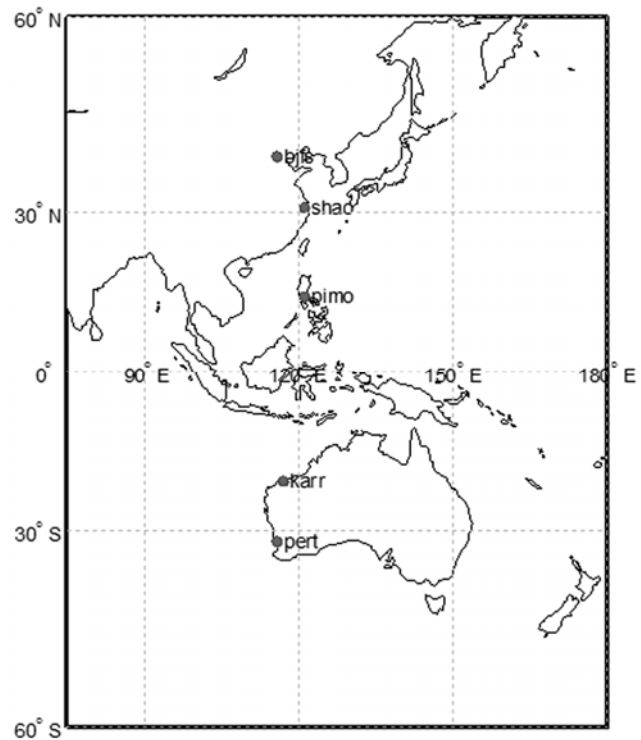


Fig. 1 — Map showing the stations selected for the study

Table 1 — Coordinates of the stations used in the present study

Station Name and Symbol	Geographic Latitude	Geographic Longitude	Geomagnetic Latitude	Dip
Fangshan (bjfs)	39.6° N	115.8° E	29.6° N	58.38°
Sheshan (shao)	30.9° N	121° E	21.2° N	46.23°
Quezon City(pimo)	14.5° N	121° E	4.9° N	16.14°
Karratha (karr)	20.9° S	117° E	30.5° S	-53.45°
Perth (pert)	31.6° S	115.8° E	41° S	-66.01°

profiles and dayside neutral composition information.

The GUVI column O/N₂ ratio is determined from O (135.6 nm) and N₂ (NBH) emissions and is estimated with 1.75°×1.75° spatial resolution²¹. The derived O/N₂ is the ratio of height-integrated O density to the height-integrated N₂ density above a reference level near the bottom of the photoelectron-excited dayglow layer (a variable altitude of approximate 140 km, above which the height-integrated density of N₂ is 10¹⁷ cm⁻²). The thermospheric O/N₂ ratio during the storm days has been collected from TIMED/GUVI. In addition we have also used the VTEC ionospheric maps downloaded from downloaded from (<http://igscb.jpl.nasa.gov/components/prods.html>).

3 Results

As we have entered the 24th solar cycle, more and more geomagnetic storms will be common. A prolonged period of southward interplanetary magnetic field brought moderate Geomagnetic Storm conditions early on 14 November (UTC), evening hours of 13 November (EST).

A Coronal Mass Ejection from the Sun was responsible for this storm that arrived to the Earth at about 10 UT on 12 November 2012. The solar wind parameters during 7-15 November 2012 are depicted in Fig. 2. On 13 November, the solar wind speed increased to 461.2 km/h and this was followed by southward turning of the B_z component of interplanetary magnetic field fluctuated to reach a maximum value of -18.2 nT on November 14. The dawn–dusk component of interplanetary electric field (IEF), E_y has been computed and shown in Fig. 3. It can be seen from Fig. 4 that, the dawn-dusk

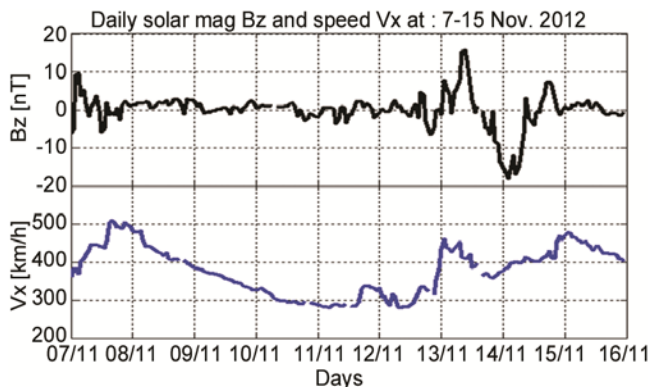


Fig. 2 — IMF B_z component (top panel) and solar wind speed (bottom panel) on 7-16 November 2012

component of IEF, E_y, calculated from $E_y = V_x B_z^{24}$. E_y is seen to oscillate from 13 to 14 November 2012, in accordance with the IMF B_z.

As suggested by Wei²⁴ under a dawn/dusk/dusk-dawn (positive/negative) IEF, the penetration electric field at the equatorial ionosphere is eastward/westward (positive/negative) on the dayside as well as westward/eastward (negative/positive) on the nightside and subsequently has a positive/negative correlation with the IEF on the dayside/nightside, respectively. We have followed the approach given by Zhao²⁵ and Wei²⁶, in which they mention the use of electric field E_y rather than the plasma bulk flow velocity V in studying the effect of PPEF, as E_y is merely a consequence of V.

Geomagnetic data for this storm are plotted in Fig. 4. This figure exhibits increase in k_p (panel a), increase in A_m (panel b), increase in maximum negative excursion of Dst (panel c) and fluctuations in AE index (panel d). The sudden storm commencement (SSC) occurred at 23:11 UT on 12 November, 2012. This was followed by SSC the geomagnetic indices k_p, a_m and AE increase rapidly. The corresponding Dst values, which is the storm time index, started decreasing and maximum negative excursion of Dst ~ -109 nT occurred on 14 November. The recovery phase of the storm started on 15 November. Our interest is to study the ionospheric parameter changes from mid latitude region to the equatorial region in the Asian sector (~115-121°E longitude sector) on 14 November. Coordinates of the stations used in this analysis are provided in Table 1.

Vertical TEC (VTEC) values for all these stations are plotted as a function of days in Fig. 5. Slant TEC measurement at one minute interval from the GPS receiver are converted into VTEC from elevation angle greater than 35° using the formula given by Rama Rao²⁷. From Fig. 5 it is clear that significant VTEC variations were obtained on 14 November 2012. Starting from the low latitude station bjfs,

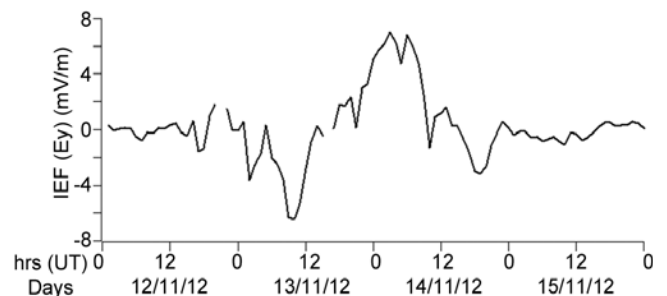


Fig. 3 — Variation of IEF E_y for 12-15 November 2012

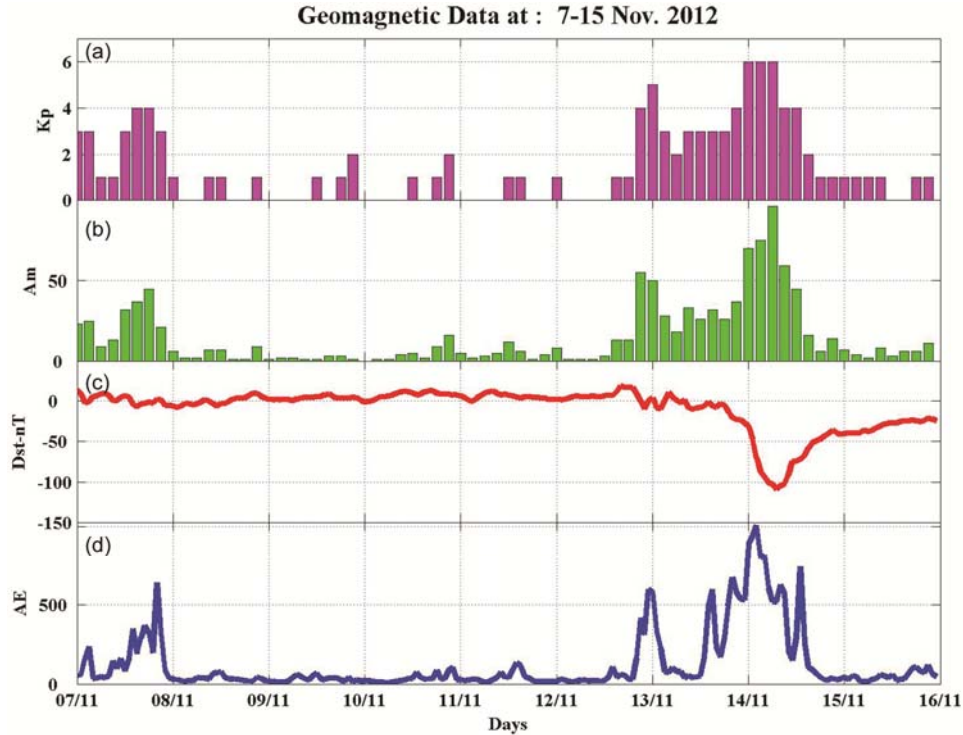


Fig. 4 — Variations in the geomagnetic activity indices (a) kp, (b) Am, (c) Dst and (d) AE index for the period 7-16 November 2012

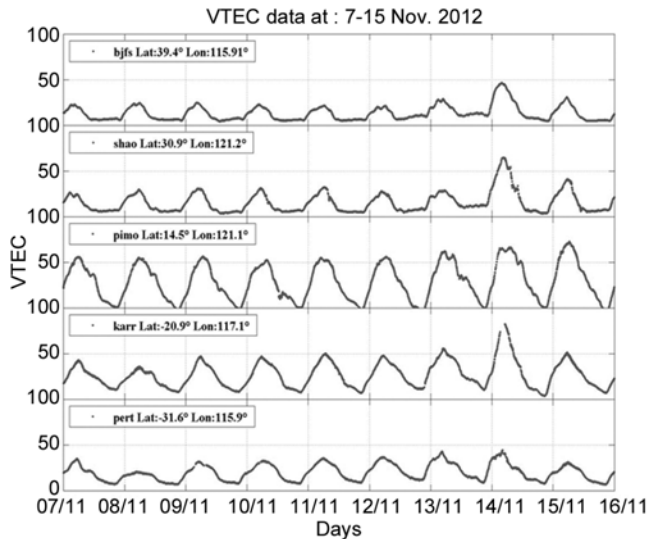


Fig. 5 — VTEC as a function of days from 7-15 November 2012 for all stations studied

VTEC values enhanced from 0 to 10 hr UT \sim 30% to 40% from the quiet time values. Moving to the equatorial region the station, shao shows even more strengthened variations \sim 50% from 0 to 12 hr UT. It is worth mentioning here that, the station shao lies in the equatorial ionization anomaly (EIA) region. No significant variation was obtained for the equatorial

station pimo. The low latitude station, karr also showed significant VTEC increase \sim 50%, from 0 to 10 hr UT. No significant variations were obtained for the mid latitude station pert. Max TEC values for the stations were observed around local noon time (13-14 hrs LT) and persist until 18-20 hr LT.

3.1 Global ionospheric TEC variations

In order to confirm the observed TEC variations we have also used the Global Ionospheric Maps which have 2 h temporal resolution obtained from a large network of GPS receivers worldwide for quiet day 9 and 11 November shown in Fig. 6. It is obvious from the figure that a clear formation of EIA started at 0 UT and further widening was observed. An intensified and latitudinal expanded EIA was noticed on 14 November from 2 hr UT to 10 hr UT with VTEC values from 80-100 TECU.

3.2 Thermospheric Response

Figure 7 shows the map of O/N₂ ratio derived from TIMED/GUVI during 11-16 November 2012. The GUVI samples once over each orbit in both the Southern and Northern hemispheres. The O/N₂ ratio was for a fixed UT. It showed enhanced ratio in the mid latitude and low latitude stations during storm conditions on 14 November. The observed increase in

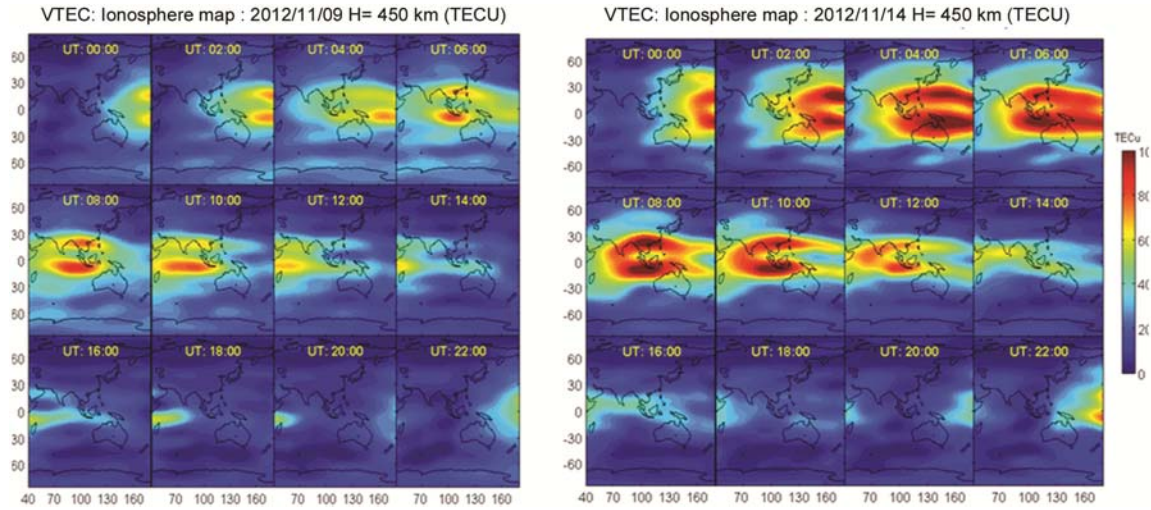


Fig.6 — VTEC ionospheric map for 9 November 2012 and 14 November 2012 downloaded from (<http://igsceb.jpl.nasa.gov/components/prods.html>)

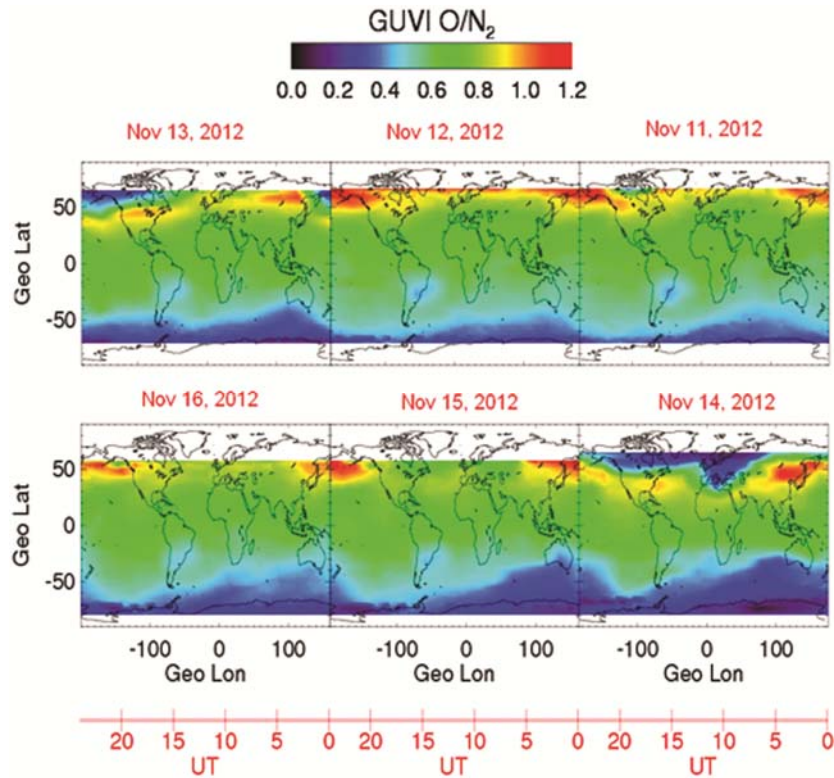


Fig. 7 — Global maps of O/N₂ ratio (from Global Ultraviolet Imager (GUVI) experiment flown on TIMED satellite for 11-16 November, 2012

TEC values at low latitude station, bjfs can be attributed to the increased O/N₂ ratio.

4 Discussion

Variation of GPS derived VTEC was considered from low to middle latitude stations for the storm of

14 November 2012. The SSC occurred on 12 November at 23:88 UT. Results clearly showed that most pronounced effect of the storm was in the EIA region. The Ey turned eastward at 16:00 UT (21:30 LT) on 13 November and remained eastward till 8:00 UT (14:30 LT) on 14 November and enhancement in

VTEC at equatorial anomaly stations, shao and karr also occurred during this period correlated with the values of E_y .

The observed variations revealed that during the main phase of the storm, PPEF modified the equatorial electric field. It is well known that during day time, prompt penetration electric field (PPEF) is eastward and enhanced the dynamo electric field. This dynamo electric field enhanced vertical $E \times B$ plasma drift with lifting the plasma to higher altitudes²⁸. At these altitudes, the production to loss ratio was greater which resulted into enhanced electron density in the dayside sector. Thus, prompt penetration electric field is associated with huge enhancement in TEC in the dayside sector¹⁵ and depletion in TEC in night side sector¹⁶. The EIA is also found to intensify in amplitude and latitude extent in the presence of PPEF¹⁷. Strong eastward PPEF produced a strong equatorial plasma fountain and plasma was lifted upward to higher latitudes. The lower TEC values at the equatorial station clearly indicated that EIA was exhibited during the storm process. The dayside ionospheric storms due to PPEFs are characterized by transport of near-equatorial plasma to higher altitudes and latitudes, forming a giant plasma fountain. These features are part of what is called the dayside ionospheric superfountain (DIS). For these southward IMFs, dusk and dawn plasma were predicted to be transported toward the dayside.

The penetration of IEF can be very fast and hence they have been called “prompt penetrating electric fields”²⁹. During very large storms, these electric fields were substantially larger than the fields associated with the normal fountain effect²². Interestingly the storm under consideration was a moderate one but could produce significant positive effect in the ionosphere. The normal equatorial fountain was modified by these electric fields leading to the superfountain effect. Under the effect of this electric field the equatorial plasma was lifted to higher altitudes, creating the so called equatorial irregularities. The equatorial ionization anomaly (EIA) region (crests located around 15° to 20° north and south) was explained by Appleton³⁰ and later by Mitra³¹. The $E \times B$ convection seems to have transported the EIA plasma to higher latitudes, as observed in the TEC increase of the stations shao and karr. This created the positive storm effect in the ionosphere.

Many researchers attribute the positive storm effect observed in the ionosphere to the

thermospheric neutral composition changes during the main phase of the storms and has been shown by model simulations^{32,33}. The downwelling of the atmosphere causes a decrease in molecular gases (or increase in $[O/N_2]$) in the F layer. The atomic oxygen being lighter is lifted faster and reaches low latitudes earlier and enhances O/O_2 and O/N_2 density ratio, increasing the VTEC²⁷ (positive ionospheric storm). From the GUVI data in Fig. 7, increased O/N_2 ratio can be seen around 30° to 40° latitude region on 14 November, 2012. The disturbances in the O/N_2 ratio penetrated up to the low latitude and not up to the equatorial latitude and therefore could not have produced the equatorial effects as seen from the TEC variations at the equatorial station pimo. Here no significant TEC variations have been observed.

Energy injection by Joule heating at the polar region and the ionosphere responses for the geomagnetic disturbances usually initiate from the polar region and then propagate to the middle and low latitudes, accompanied with the modification of the local atmosphere conditions, causing ionosphere anomalies which are comprehensively observed and discussed. The expansion of the equatorial ionization anomaly (EIA), further leading to hemisphere asymmetry in response to the storm. Also, the GUVI observations do not show enhanced O/N_2 ratio in the southern hemisphere for pert station. All these effects explain the absence of any significant variation in TEC at pert station.

5 Conclusion

In this paper, we have analyzed and presented the ionospheric storm effect on the basis of the observation of VTEC data obtained from GPS satellites in the Asian sector during the moderate storm on 14 November 2012. The main results can be summarized as:

- i. The GPS TEC observations showed pronounced positive storm effects in the Asian sector (~117° E) during the main phase of the storm. There was significant increase in VTEC from the EIA region up to low latitude region.

- ii. The enhancements in TEC centered at the northern and southern EIA region could be produced by the enhanced fountain effect due to the PPE during the southward turning of IMF Bz. The EIA was shown to be intensified during the main phase of the storm in the daytime. The ionospheric plasma was

lifted up by the vertical $E \times B$ drift at the dip equator and went down along geomagnetic lines of force to both sides of the equator. Plasma located slightly away from the equator was not only lifted upward but also displaced to higher latitudes. The penetration of storm time electric fields was fast and capable of enhancing the normal fountain effect.

iii. To study the thermospheric changes during storm time the O/N_2 ratio was used. Increase in O/N_2 was observed in the low latitude region and not near the equator. This increase was not responsible for the positive storm effects that were observed. It is possible that the perturbations in the O/N_2 ratio did not penetrate to much lower latitudes because of the moderate geomagnetic storm.

iv. The observations presented in this paper show that the morphology of the low-latitude ionosphere can vary dramatically even in case of moderate geomagnetic storms.

Acknowledgement

Authors would like to thank the International GNSS Service (IGS) for providing VTEC maps and also to the Telecommunications/ICT for Development (T/ICT4D) Laboratory of the Abdus Salam International Centre for Theoretical Physics, Trieste.

References

- 1 Mendillo M, *Nature*, 234 (1971) 23.
- 2 Fuller Rowell T J, Codrescu M V, Rishbeth H, Moffett R J & Quegan S, *J Geophys Res*, 101 (1996) 2343.
- 3 Buonsanto M J & Fuller-Rowell T J, *EOS Transactions American Geophysical Union*, 78 (1997) 1.
- 4 Buonsanto M J, *Space Sci Rev*, 88 (1999) 563.
- 5 Danilov A D, *J. Atmos. Solar-Terr Phys*, 63 (2001) 441.
- 6 Belehaki A & Tsagouri I, *Physics and Chemistry of the Earth*, 26 (5) (2001) 309.
- 7 Dabas R S, Das R M, Vohr V K & Devasia C, *Ann Geophysicae*, 24 (1) (2006) 97.
- 8 Buresova D, Lastovicka J & deFranceschi G, In: Lilensten, J.(Ed.); *Space Weather Research towards Applications in Europe*. Springer, Dordrecht (2007) 185.
- 9 Namba S & Maeda K I, *Radio Wave Prop*, (1939) 86.
- 10 Balan N & Bailey G J, *J Geophys Res*, 100, A11, 21 (1995) 421.
- 11 Fejer B G, Jensen J W, Kikuchi, T, Abdu M A & Chau J L, *J Geophys Res*, 112 A10304 (2007) 1.
- 12 Scherliess L & Fejer B G, *J Geophys Res*, 102(A12) (1997) 24.
- 13 Richmond A D, Peymirat C & Roble R G, *J Geophys Res*, 108(A3) (2003) 1118.
- 14 Rastogi R G & Klobuchar J A, *J Geophys Res*, 95 (1990) 19,045.
- 15 Tsurutani B, Mannucci A, Iijima B, Ali Abdu M, Sobral J H A, Gonzalez W, Guarneri F, Tsuda T, Saito A, Yumoto K, Fejer B, Fuller-Rowell T J, Kozyra J, Foster J C, Coster A & Vasyliunas V M, *J Geophys Res*, (2004) 109.
- 16 Abdu M A, Maruyama T, Batista I S, Saito S & Nakamura M, *J Geophys Res*, 112 A10306 (2007) 1.
- 17 Veenadhari B, Alex S, Kikuchi T, Shinbori A, Singh R & Chandrasekhar E, *J Geophys Res* 115 A03305 (2010) 1.
- 18 Huang C S, Foster J C, Kelley M C, *J Geophys Res*, 110 A11309 (2005) 1.
- 19 Fejer B G, Paula E R de, Heelis R A & Hanson W B, *J Geophys Res*, 100(A4) (1995) 5769.
- 20 Gaurav B, Bag T & Sunil Krishna M V, *J Atmos and Solar-Terrestrial Phys*, 168 (2018) 8.
- 21 Christensen A B, Paxton L J, Avery S, Craven J, Crowley G, Humm D C, Kil H, Meier R R, Meng C I, Morrison D, Ogorzalek B S, Straus P, Strickland D J, Swenson R M, Walterscheid R L, Wolven B & Zhang Y, *J Geophys Res*, 108 (A12) (2003) 1451.
- 22 Yee J H, Elsayed R, Andrew B, Christensen T, Killeen L, Russell J M & Thomas N, *Johns Hopkins Apl Technical Digest*, 24(2) (2003).
- 23 Yee J H, Cameron, G E & Kusnierkiewicz D Y, *SPIE* 3756 (1999) 244.
- 24 Wei Y, Hong M, Wan W, Du A, Lei J, Zhao B, Wang W, Ren Z & Yue X, *Geo Phys Res Letters*, 35 (2008) L02102.
- 25 Zhao B, Wan W, Tschu K, Igarashi K, Kikuchi T, Nozaki K, Watari S, Li G, Paxton L J, Liu L, Ning B, Liu, J Y, Su, S Y & Harold P, *J Geophys Res*, 113 (2008) 1.
- 26 Wei Y, Wan W, Zhao B, Hong M, Ridley A, Ren Z, Fraenz M, Dubinin E & He M, *J Geophys Res*, 117 (2012) 1.
- 27 Rama Rao PVS, Gopi Krishna S, Niranjan K & Prasad DSVVD, *Ann Geophys*, 24 (2006) 3279.
- 28 Rastogi R G. & Klobuchar J A, *J Geophys Res*, 95 (1990) 19,045.
- 29 Tsurutani B T, Verkhoglyadova O P, Mannucci A J, Saito A, Araki T, Yumoto K, Tsuda T, Abdu M A, Sobral J H A & Gonzalez W D, McCreadie H, Lakhina G S & Vasyli V M, *J Geophys Res*, 113 (2008) 1.
- 30 Appleton EV, *Nature*, 157 (1946) 691.
- 31 Mitra S K, *Nature*, 158 (1946) 668.
- 32 Rishbeth H, Fuller-Rowell T J & Rees D, *Planet Space Sci*, 35 (1987) 1157.
- 33 Burns A G, Killeen T L, Deng W, Carignan G R & Roble R G, *J Geophys Res*, 100 (14) (1995) 673.